A polarized liquid crystal lens with electrically switching mode and optically written mode

Hung-Shan Chen[1], Yi-Hsin Lin[1]*, Chia-Ming Chang[1], Yu-Jen Wang[1], Abhishek Kumar Srivastava[2], Jia Tong Sun[2], and Vladimir Grigorievich Chigrinov[2]

[1]Department of Photonics, National Chiao Tung University, Hsinchu, Taiwan
[2]State Key Lab on Advanced Displays and Optoelectronics, Department of Electronic and Computer Engineering, Hong Kong University of Science and Technology, Hong Kong, China
*Corresponding author: yilin@mail.nctu.edu.tw

ABSTRACT

A polarized liquid crystal (LC) lens composed of a LC layers as a polarization switch and a liquid crystal and polymer composites lens (LCPC lens) is demonstrated with electrically switching (ES) mode and optically rewritten (ORW) mode. The lens power of LCPC lens is related to a polarization state of light modulated by the LC layer whose orientations are manipulated either electrically or optically. As a result, the LC lens is not only electrically switchable, but also optically rewritable. Each mode, ES mode or ORW mode, exhibits two discrete lens powers (-1.39 Diopter and +0.7 Diopter). The demonstrated aperture size is 10 mm. The detail optical mechanism is also discussed. The Modulation Transfer Function (so-called MTF) of the lens is measured as well. In addition, the image performance and the dispersion of the LC lens are investigated. Such a polarized LC lens could be a special switch in optical systems due to dual operation modes.

Keywords: Bistable, Ophthalmic Lens, Optically Rewrite, Liquid Crystal Lens, Polarization switch

1. INTRODUCTION

Electrically tunable focusing liquid crystal (LC) lenses have many applications in optical systems.[1-10] Most LC lenses consume electric power in order to reorient LC directors. For many applications, such as ophthalmic lenses, bistability of a lens is required. Optically rewritable (ORW) alignment layer allowing bistable alignment for LC molecules is applied to applications, such as e-paper, gratings, and Fresnel zone lenses.[11-15] However, the Fresnel zone lenses are limited by diffraction efficiencies and imaging qualities. Recently, we propose a negative lens with large aperture size (~10mm) by integrating a polarization switch of ferroelectric liquid crystal (FLC) with a polymeric lens, liquid crystal and polymer composite (LCPC) lens.[10] However, optical properties of FLC are chromatic which means the wavelength dependency, and it shows focusing ability as a negative lens only. Recently, we proposed and demonstrated a polarized bifocal switch based on liquid crystals operated electrically and optically which exhibits both

Emerging Liquid Crystal Technologies X, edited by Liang-Chy Chien, Harry J. Coles, Hirotsugu Kikuchi, Ivan I. Smalyukh,
Proc. of SPIE Vol. 9384, 938413 · © 2015 SPIE · CCC code: 0277-786X/15/$18 · doi: 10.1117/12.2082622

positive and negative lens power with large aperture size (~10mm) in terms of a combination of a polarization switch and a different liquid crystal polymer composite (LCPC) lens.[16] The proposed LC lens not only shows optically tunable bistability, but also electrically switchability with a low driving voltage (<$5V_{rms}$). However, the detail optical mechanism how polarization rotates and how image formations of rotated polarizations are have not been discussed yet. The image qualities are not addressed either. In this paper, the operating mechanism based on Jones Matrix approach is addressed. The imaging qualities, such as MTF and chromatic properties of the proposed LC lens, are demonstrated. This study opens a window for developing bistable LC lenses, which makes lots of application more practical, such as imaging systems for portable device, wearable devices, and ophthalmic lenses.

2. STRUCTURE AND OPERATING PRINCIPLE

The structure and operating principles of the polarized LC lens are illustrated in Fig 1. The LC lens consists of three glass substrates, four alignment layers, one photo alignment layer, two ITO layers, one liquid crystal polymer composite (LCPC) layer, a LC layer as the polarization switch and a polarizer. The LCPC layer consists of two polymeric sub-lenses, a plano-concave LCPC lens and a plano-convex LCPC lens. The effective optic axes of those two LCPC lenses are along y-direction and x-direction for plano-concave LCPC lens and plano-convex LCPC lens, respectively. The polarization switch composed of a layer of nematic liquid crystals sandwiched between two Indium-Tin-Oxide (ITO) glass substrates coated with a photoalignment layers and a typical alignment layer (i.e. non-photoalignment layer). The typical alignment layer (i.e. non-photoalignment layer) was polyimide (PI) and the rubbing direction was along y-direction. The material of the photoalignment layer was sulfonic azo dye. The aligned direction of the photo-alignment direction is perpendicular to the linear polarization of exposed UV light. Moreover, the alignment direction of the photo-alignment layer is rewritable according to the UV dose as well as directions of UV polarization, as shown in Fig. 1(a). In the absence of the electric field, the x-linearly polarized light incident to the LC layer is converted to y-linearly polarized light due to the twist nematic (TN) configuration (i.e. a twisted angle of 90 degree in Fig. 1(b)). The polarization of incident light is switched by the LC layers first and then propagates to the LCPC layers. The lens powers of the LCPC lenses are related to the polarization of incident light. Assume that R is the radius of curvature of the interface between two LCPC lenses, n_o is ordinary refractive index of the LCPC lenses and n_e is extraordinary refractive index of the LCPC lenses. Two LCPC layer are actually made of same materials, but the effective optic axes are orthogonal to each other. Thereafter, the y-linearly polarized light experiences the lens powers of $(n_o - 1)/R$ and $(1 - n_e)/R$ when light passes through top and bottom LCPC lenses, respectively. The total lens power is the summation of two lens powers, which leads to $(n_0 - n_e)/R$ <0 as $n_e > n_o$. As a result, the polarized LC lens behaves as a negative lens, as shown in Fig. 1(b). When the applied voltage (V) exceeds the threshold voltage (V_{th}), the LC molecules are reoriented along z-direction, as illustrated in Fig. 1(c). The x-linearly polarized light keeps the same polarization state due to light propagation along optic axes of the LC layer. The x-linearly polarized light then experiences a total lens power of $(n_e - n_0)/R$ >0. The polarized LC lens behaves as a positive lens. Figs. 1(a) 1(b), and 1(c) are operated in the electrically-switching mode (ES mode) of the LC lens. In Fig. 1(a), the photoalignment layer aligns LC molecules along

x-direction by removing the polarizer and then y-linearly polarized UV light (λ=365 nm) is exposed to the photoalignment layer. Similarly, we expose x-linearly polarized UV light to the photoalignment layer in Fig. 1(d) and LC molecules near the photoalignment layer are aligned along y-direction. Thus, the twist of the LC molecules of the LC layer is no longer sustained which are all aligned along y-direction. In Fig. 1(e), the x-linearly polarized light is o-wave to the LC layer. The polarization thus remains x-linearly polarized during propagation. As a result, the polarized LC lens is a positive lens with a lens power of $(n_0 - n_e)/R$. In Figs. 1(b) and 1(e), the proposed LC lens is operated in the optically-rewritable mode (ORW mode). Therefore, the LC lens is not only electrically switchable, but also optically rewritable. In addition, only two discrete lens powers exist in both ES mode and ORW mode. The difference of two discrete lens powers is $2\times(n_e - n_o)/R$.

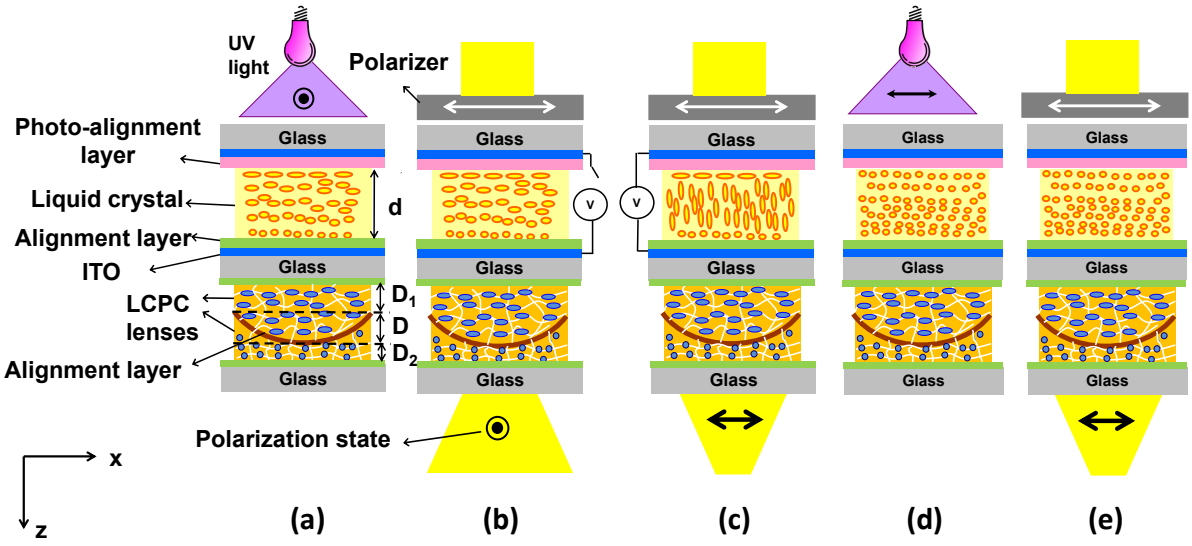

Fig 1. The structure and operating principles of the polarized LC lens.

The polarization of the unpolarized light is composed of rapid succession of different polarizations and each random polarization ($\vec{E}_{in}$) can be decomposed as x- and y-linearly polarized light with randomly relative phase difference, as written in (1).

$$\vec{E}_{in} = A_x e^{i\phi_{x0}} \cdot \hat{x} + A_y e^{i\phi_{y0}} \cdot \hat{y} \tag{1}$$

where A_x and A_y represents the amplitude of the electric field, ϕ_{x0} and ϕ_{y0} are the phase term of the electric field. After light passing through the polarizer whose transmissive axis is along x-direction, the polarization can be expressed as

$$\vec{E}_{in}' = A_x e^{i\phi_{x0}} \cdot \hat{x} \tag{2}$$

The Jones Matrix of the polarization switch can be expressed as: [17]

$$M_{PS} = R(-\phi)\left[e^{-i\frac{k(n_e+n_o)d}{N}} \begin{pmatrix} e^{-\frac{\Gamma}{2N}} & 0 \\ 0 & e^{\frac{\Gamma}{2N}} \end{pmatrix} R(\frac{\phi}{N}) \right]^N = e^{-ik(n_e+n_o)d} R(-\phi)\left[\begin{pmatrix} e^{-\frac{\Gamma}{2N}} & 0 \\ 0 & e^{\frac{\Gamma}{2N}} \end{pmatrix} R(\frac{\phi}{N}) \right]^N$$
$$= e^{-ik(n_e+n_o)d} \begin{pmatrix} \cos\phi & -\sin\phi \\ \sin\phi & \cos\phi \end{pmatrix} \begin{pmatrix} \cos \mathrm{X} - i\frac{\Gamma \sin \mathrm{X}}{2\mathrm{X}} & \phi\frac{\sin \mathrm{X}}{\mathrm{X}} \\ -\phi\frac{\sin \mathrm{X}}{\mathrm{X}} & \cos \mathrm{X} + i\frac{\Gamma \sin \mathrm{X}}{2\mathrm{X}} \end{pmatrix} \quad (3)$$

where ϕ is the twist angle of the director, $\Gamma = \frac{2\pi}{\lambda} \times \Delta n \times d$ is the phase retardation, d is the thickness of the LC layer, and $\mathrm{X}^2 = \phi^2 + \frac{\Gamma^2}{4}$. We assume $\phi \gg \Gamma$ to avoid incomplete polarization rotation, therefore the polarization switch M_{PS} can be expressed as:[17]

$$M_{PS} = e^{-ik(n_e+n_o)d} \begin{pmatrix} \cos\phi & -\sin\phi \\ \sin\phi & \cos\phi \end{pmatrix} \begin{pmatrix} e^{-i\frac{\Gamma}{2}} & 0 \\ 0 & e^{i\frac{\Gamma}{2}} \end{pmatrix}. \quad (4)$$

Assume the phase profile of the LCPC layers for the x-direction linearly polarized light is:

$$k \times n_{e,LCPC} \times (D_1 + D - \frac{r^2}{2R}) + k \times n_{o,LCPC} \times (D_2 + \frac{r^2}{2R}) \quad (5)$$

R is the curvature of the interface between two LCPC lenses, D is the thickness of curvature of the LCPC layer (see Fig. 1(a)), r is $\sqrt{x^2 + y^2}$, $n_{e,LCPC}$ and $n_{o,LCPC}$ respectively represent extraordinary refractive index and ordinary refractive index of the LCPC layer. Similarly, assume the phase profile of the LCPC layers for the y-direction linearly polarized light is:

$$k \times n_{o,LCPC} \times (D_1 + D - \frac{r^2}{2R}) + k \times n_{e,LCPC} \times (D_2 + \frac{r^2}{2R}) \quad (6)$$

Then we can regard the LCPC layer as a wave retarder as:

$$M_{LCPC}(r) = \begin{pmatrix} e^{-i[k \times n_{e,LCPC} \times (D_1 + D - \frac{r^2}{2R}) + k \times n_{o,LCPC} \times (D_2 + \frac{r^2}{2R})]} & 0 \\ 0 & e^{-i[k \times n_{o,LCPC} \times (D_1 + D - \frac{r^2}{2R}) + k \times n_{e,LCPC} \times (D_2 + \frac{r^2}{2R})]} \end{pmatrix} \quad (7)$$

Then the output electric field of the light can be derived by Jones calculus:

$$\vec{E}_{out}(r) = M_{LCPC}(r) \cdot M_{PS} \cdot \vec{E}_{in}' \quad (8)$$

In ES mode, the polarization switch without applied voltage (ES-off) can be expressed as ($\phi = \frac{\pi}{2}$)

$M_{PS}(ES-off) = e^{-ik(n_e+n_o)d}\begin{pmatrix}0 & -1\\ 1 & 0\end{pmatrix}\begin{pmatrix}e^{-i\frac{\Gamma}{2}} & 0\\ 0 & e^{i\frac{\Gamma}{2}}\end{pmatrix}$, therefore the output electric field can be expressed as:

$$\begin{aligned}\vec{E}_{out,ES-off}(r) &= A_x e^{i\phi_{x0}}\cdot e^{-ik(n_e+n_o)d}\cdot e^{-i\frac{\Gamma}{2}}\cdot e^{-i[k\times(n_{o,LCPC})\times(D_1+D-\frac{r^2}{2R})+k\times(n_{e,LCPC})\times(D_2+\frac{r^2}{2R})]}\cdot\hat{y}\\ &= A_x e^{i[\phi_{x0}-2kn_e d-k(n_{o,LCPC})\times(D_1+D)-k(n_{e,LCPC})\times(D_2)]}\cdot e^{-ik\times(n_e-n_o)\times(\frac{r^2}{2R})}\cdot\hat{y}\end{aligned} \quad (9)$$

Similarly, in ES mode, the polarization switch with applied voltage (ES-on) can be expressed as $M_{PS}(ES-on) = e^{-ik(n_e+n_o)d}\begin{pmatrix}1 & 0\\ 0 & 1\end{pmatrix}\begin{pmatrix}1 & 0\\ 0 & 1\end{pmatrix}$, therefore the output electric field can be expressed as:

$$\begin{aligned}\vec{E}_{out,ES-on}(r) &= A_x e^{i\phi_{x0}}\cdot e^{-ik(n_e+n_o)d}\cdot e^{-i[k\times(n_{e,LCPC})\times(D_1+D-\frac{r^2}{2R})+k\times(n_{o,LCPC})\times(D_2+\frac{r^2}{2R})]}\cdot\hat{x}\\ &= A_x e^{i[\phi_{x0}-k(n_e+n_o)d-k(n_{e,LCPC})\times(D_1+D)-k(n_{o,LCPC})\times(D_2)]}\cdot e^{-ik\times(n_o-n_e)\times(\frac{r^2}{2R})}\cdot\hat{x}\end{aligned} \quad (10)$$

In ORW mode, the polarization switch after exposed to x-direction linearly polarized UV light can be expressed as $M_{PS-ORW} = e^{-ik(n_e+n_o)d}\begin{pmatrix}1 & 0\\ 0 & 1\end{pmatrix}\begin{pmatrix}e^{-i\frac{\Gamma}{2}} & 0\\ 0 & e^{i\frac{\Gamma}{2}}\end{pmatrix}$, therefore the output electric field can be expressed as:

$$\begin{aligned}\vec{E}_{out,ORW}(r) &= A_x e^{i\phi_{x0}}\cdot e^{-ik(n_e+n_o)d}\cdot e^{-i\frac{\Gamma}{2}}\cdot e^{-i[k\times(n_{e,LCPC})\times(D_1+D-\frac{r^2}{2R})+k\times(n_{o,LCPC})\times(D_2+\frac{r^2}{2R})]}\cdot\hat{x}\\ &= A_x e^{i[\phi_{x0}-2kn_e d-k(n_{o,LCPC})\times(D_1+D)-k(n_{e,LCPC})\times(D_2)]}\cdot e^{-ik\times(n_o-n_e)\times(\frac{r^2}{2R})}\cdot\hat{x}\end{aligned} \quad (11)$$

In Eq. (9), (10), and (11), the first phase term can be ignored because it is independent of position. According to the approximation of thin lens, the second phase term equals to phase transformation of $e^{-jk\times\frac{r^2}{2\times f}}$, where f is focal length. Therefore, lens power (P=1/f) satisfies: $P(ES-off)=\frac{\Delta n}{R}$, $P(ES-on)=\frac{-\Delta n}{R}$, and $P(ORW)=\frac{-\Delta n}{R}$. There are two ways to adjust the lens power of the polarized LC lens: ES-mode and ORW-mode. When operating in ES-mode, the output wave can be switched between E_{out}(ES-off) and E_{out}(ES-on) by applying voltage. For ORW-mode, the output wave can be switched between E_{out}(ES-off) and E_{out}(ORW) by UV exposure. The tunable range of the lens power ΔP is:

$$\Delta P = P(ES-off)-P(ES-on) = P(ES-off)-P(ORW) = \frac{2\Delta n}{R} \quad (12)$$

3. EXPERIMENT RESULTS AND DISCUSSION

To observe the phase profile of the LCPC lens, we placed the LCPC lens under crossed polarizers. The green laser (λ=532nm) and red laser (λ=633nm, from Meredith Instruments) were adopted to test the wavelength-dependent phase profile. The rubbing directions of two LCPC lenses were 45° and 135° with respect to one transmission axis of the polarizers. The observed images at different wavelengths are shown in Fig. 2(a) and Fig. 2(b). In Fig. 2(a), the images

with concentric rings indicate the phase profiles of the LCPC lenses, where two adjacent bright fringes or dark fringes represent phase shift of 2π radians. As we can see in Fig. 2(a) and Fig. 2(b), both phase profiles are symmetric. The phase difference between the center and the edge is $N \cdot 2\pi$ radians, where N is the number of pairs of bright fringes between the center and the edge. Under the thin lens approximation (i.e. $e^{i\frac{k\times r^2\times(n-1)}{2R}} = e^{i\frac{k\times r^2}{2f}}$), we can calculate the lens power of the LCPC lenses (P): $\Delta P = \frac{2\times N\times\lambda}{r^2}$ .The calculated lens power is around 2.3D and 2.25D for the green light and the red light, respectively. The LCPC lenses show small chromatic behavior. To measure lens power, we adopted the Shack Hartmann wavefront sensor. From experiments, the polarized LC lens shows the positive lens power of 0.69D and the negative lens power of -1.38D under red light.[16] To test the sample of the polarization switch, we measured the voltage-dependent transmittance (so-called VT curve) of the polarization switch under ES mode. The polarization switch was located between two crossed polarizers, and the VT curve was measured under two wavelengths (λ=543nm and 633nm). Referring to Fig. 2(c), we measured the transmittance of the polarization switch as a function of applied voltage. The transmittance of the polarization switch shows bright state at voltage off state which is the case of typical TN mode. At $0V_{rms}$, the transmittance increase for both green and red light. This is a result of incomplete polarization rotation of the polarization switch, which is also known as the 1/λ dependence of the Mauguin condition.[17] After $6V_{rms}$, both the transmittances in Fig. 2(c) are low, which indicates the LC directors are all reoriented in the z-direction.

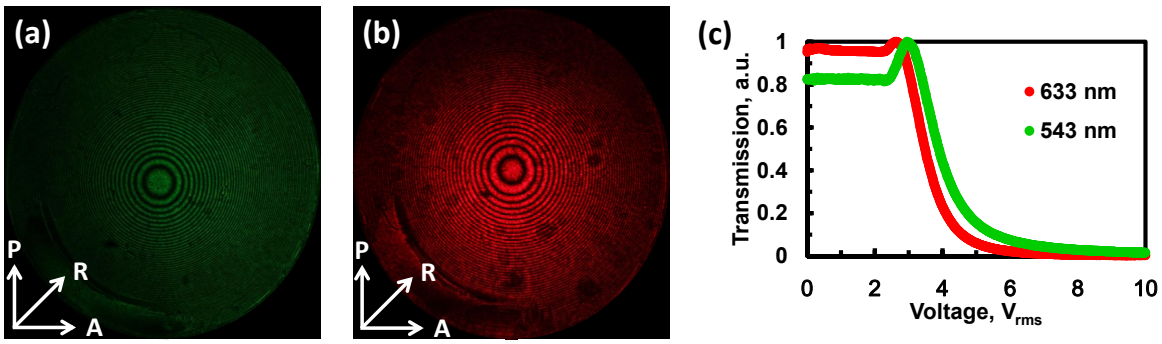

Fig. 2 Images of the LCPC layer under crossed polarizers at (a)λ=532 nm and (b)λ=633 nm. P and A are transmissive axes of the polarizer and the analyzer. R is the rubbing directon. (c) Voltage-dependent transmittance the LC layer at different wavelengths.

To evaluate the image qualities of the polarized LC lenses, the MTF measurement using a resolution chart was performed. The polarized LC lens was attached in front of a camera (Canon 500D, Canon EF-S 18-55mm f/3.5-5.6 IS). A resolution chart (USAF 1951) with difference spatial frequencies was placed in front of the polarized LC lens. An iris with an aperture size of 10mm was placed in front of the polarized LC lens as an aperture stop. The distance between the resolution chart and the polarized LC lens is the objective distance. We recorded the images with and without the polarized LC lens. We also replaced the polarized LC lens with standard spherical glass lens (Topcon) and took photos

for comparison. The images were then converted to the spatial distribution of the brightness by using software (MATLAB). The measured contrast (or MTF) of the polarized LC lens as a function of resolution is plotted in Fig. 3. Both of standard spherical glass lens and the polarized LC lens degrade imaging performance slightly. When contrast was 0.5, the spatial frequencies of MTF were 6.08 lp/mm and 6.21 lp/mm for the negative and the positive lens, respectively. Compared to the standard spherical glass lens (8.99lp/mm @ 0.75D and 10.29 lp/mm @ -1.5D; from Topcon). The negative lens shows larger degradation of MTF comparing to the positive lens of the polarized LC lens. The reason why the degradation of MTF is larger as a negative lens might because the polarization direction of the incident light was not totally rotated into the y-direction at V=0. The incomplete polarization rotation of light at different wavelengths is also addressed in Fig. 2(c), which results in double images and then degrades the MTF of the negative lens. To further improve the chromatic properties of incomplete polarization rotation, we can adopt the cell gap of the polarization switch part larger than 10 micron, or satisfy the 1st or 2nd minimum conditions of TN cell, or add the compensation films.[17]

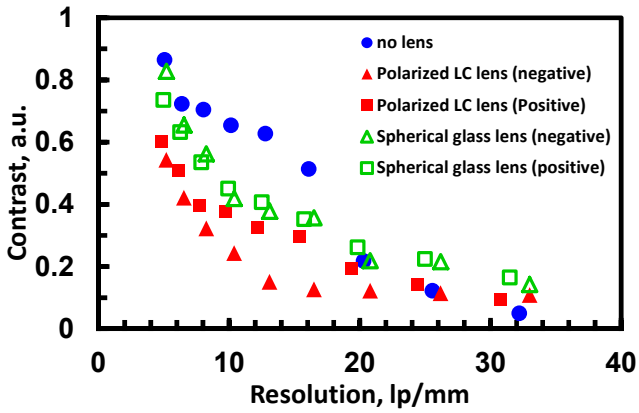

Fig. 3 The measured contrast (or MTF) as a function of spatial frequency(resolution).

To demonstrate the image quality and to prove the tunable lens power of the polarized LC lens, we measured the image performance of the polarized LC lens. The polarized LC lens was still attached on the camera and took photos directly under an ambient white light. Two different objects were placed at 400 cm, and 40 cm away from the polarized LC lens. In Fig. 4(a) and 4(b), the target at 400 cm and at 40 cm are clear at $V=0V_{rms}$ and $V=5V_{rms}$, respectively. Then, the polarized LC lens was exposed to the polarized UV light. The target at 40 cm became clear without applied voltage, as shown in Fig. 4(c). As a result, the polarized LC lens could be operated in ORW mode and in ES mode. As a result, people with myopia-presbyopia can see farther and see nearer when the polarized LC lens was operated as a positive or a negative lens. According to the results in Fig. 4, the total tunable lens power is 1/0.4-1/4=2.25D, which is closed to the result obtaining from phase profiles. Theoretically, based on Eq.(12), the total tunable lens power should be $2\times(n_{e,LCPC}-n_{o,LCPC})/R = 2\times 0.134/0.115 = 2.33D$ which is larger than the experimental results. As to the response time, it is around 20 ms and 23 ms for the rise time and fall time of ES mode with applied $5V_{rms}$, respectively.

The response time of ORW mode is around 20 sec, depends on UV intensity.

Fig. 4 The image performances of the polarized LC lens under ambient white light. (a) and (b) are operated in ES mode, while (a) and (c) are operated in ORW mode

From the experimental results, the discrepancy between the positive lens and negative lens also indicate the structure deviation from the original design, where the absolute magnitude of lens power should be similar for negative and positive lens. It is due to the thickness uniformity arising from fabrication process of the LCPC lenses, such as the induced thickness of alignment layer between the interfaces of the two LCPC lenses, as shown in Fig. 5. In Fig. 5, the thick alignment layer PI could induce two different curvatures R_1 and R_2 and also a new lens power from the middle PI layer. We assume that lens power is composed of three different lens powers, then the positive lens P_x' can be expressed as: $P_x' = \frac{n_{e,LCPC} - n_{PI}}{R_1} + \frac{n_{PI} - n_{o,LCPC}}{R_2} = 0.69D$ and the negative lens P_y' can be expressed as: $P_y' = \frac{n_o - n_{PI}}{R_1} + \frac{n_{PI} - n_e}{R_2} = -1.38D$, where $n_{e,LCPC}$, $n_{o,LCPC}$ and n_{PI} represents the extraordinary refractive index, ordinary refractive index of the LCPC lenses and the refractive index of the PI. From our experiment, we can assume that the curvature R_2 equals to the original R=115mm from the standard spherical glass mold. Then we can solve the simultaneous equations above to obtain the curvature R_1=150mm, and n_{PI}=1.42. Then we can use sag height to calculate the thickness of PI which is around 25 μm at the center of the polarized LC lens. To further minimize the discrepancy of the lens powers, we can adjust the fabrication process and materials, such as the spin coating speed and viscosity of the PI.

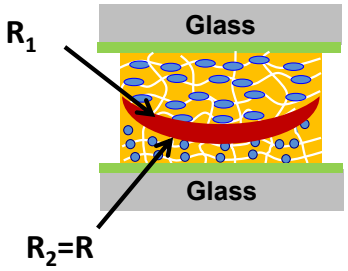

Fig. 5 The illustration actual structure of the LCPC layer. The thick middle PI layer introduces extra curvatures to affect the lens power.

4. CONCLUSION

A polarized liquid crystal (LC) lens composed of a LC layers as a polarization switch and a LCPC layer is demonstrated which can be operated in electrically switching (ES) mode and optically rewritten(ORW) mode. The polarized LC lens is not only electrically switchable, but also optically rewritable. We have discussed the operating mechanism of the polarized LC lens. Two discrete lens powers (-1.39 Diopter or +0.7 Diopter) can be obtained in both ES mode and ORW mode. The MTF and imaging performance of the polarized LC lens is also demonstrated. We believed that the analysis of such LC lens paved a way for deeper understandings of the imaging quality of imaging systems. Such a polarized LC lens can not only be applied to ophthalmic lenses but also to special switch in optical systems.

5. REFERENCE

[1] S. Sato, "Liquid-crystal lens-cells with variable focal length," Jpn. J. Appl. Phys. **18**, 1679-1684 (1979).

[2] Y. H. Lin, and H. S. Chen, "Electrically tunable-focusing and polarizer-free liquid crystal lenses for ophthalmic applications," Opt. Express **21**, 9428-9436 (2013).

[3] Y. H. Lin, M. S. Chen, and C. H. Lin, "An electrically tunable optical zoom system using two composite liquid crystal lenses with a large zoom ratio," Opt. Express **19**, 4717-4721 (2011).

[4] H. S. Chen, and Y. H. Lin, "An endoscopic system adopting a liquid crystal lens with an electrically tunable depth-of-field," Opt. Express **21**, 18079-18088 (2013).

[5] Y. H. Lin, H. S. Chen, H. C. Lin, Y. S. Tsou, H. K. Hsu, and W. Y. Li, "Polarizer-free and fast response microlens arrays using polymer-stabilized blue phase liquid crystals," Appl. Phys. Lett. **96**, 113505 (2010).

[6] G. Li, P. Ayras, S. Honkanen, and N. Peyghambarian, "High-efficiency switchable flat diffractive ophthalmic lens with three-layer electrode pattern and two-layer via structures," Appl. Phys. Lett. **90**, 111105 (2007).

[7] H. Ren, and S. T. Wu, "*Introduction to Adaptive Lenses"* (John Wiley & Sons) (2012).

[8] C. W. Fowler, and E. S. Pateras, "Liquid crystal lens review," Ophthalmic Physiol Opt. **10**, 186-194 (1990).

[9] H. C. Lin, M. S. Chen, and Y. H. Lin, "A review of electrically tunable focusing liquid crystal lenses,," Trans. Electr. Electron Mater. **12**, 234-240 (2011).

[10] H. S. Chen, Y. H. Lin, A. K. Srivastava, V. G. Chigrinov, C. M. Chang, and Y. J. Wang, "A large bistable negative lens by integrating a polarization switch with a passively anisotropic focusing element," Opt. Express **22**, 13138-13145 (2014).

[11] S. Y. Huang, T. C. Tung, H. C. Jau, J. H. Liu, and A. Y. G. Fuh, "All-optical controlling of the focal intensity of a liquid crystal polymer microlens array," Appl. Opt. **50**, 5883-5888 (2011).

[12] X. Q. Wang, F. Fan, T. Du, A. M. W. Tam, Y. Ma, A. K. Srivastava, V. G. Chigrinov, and H. S. Kwok, "Liquid crystal Fresnel zone lens based on single-side-patterned photoalignment layer," Appl. Opt. **53**, 2026-2029 (2014).

[13] S. Y. Huang, T. C. Tung, C. L. Ting, H. C. Jau, M. S. Li, H. K. Hsu, and A. Y. G. Fuh, " "Polarization-dependent optical tuning of focal intensity of liquid crystal polymer microlens array," Appl. Phys. B **104**, 93-97 (2011).

[14] L. C. Lin, H. C. Jau, T. H. Lin, and A. Y. G. Fuh, "Highly efficient and polarization-independent Fresnel lens based on dye-doped liquid crystal," Opt. Express **15**, 2900-2906 (2007).

[15] X. Q. Wang, A. K. Srivastava, V. G. Chigrinov, and H. S. Kwok, "Switchable Fresnel lens based on micropatterned alignment," Opt. Lett. **38**, 1775-1777 (2013).

[16] H. S. Chen, Y. H. Lin, C. M. Chang, Y. J. Wang, A. K. Srivastava, J. T. Sun, and V. G. Chigrinov, "A polarized bifocal switch based on liquid crystals operated electrically and optically," J. Appl. Phys. **117**, 044502 (2015).

[17] P. Yeh, and C. Gu, "Optics of Liquid Crystal Displays" (Wiley, 2nd edition) (2010).